EUROPEAN ORGANIZATION FOR NUCLEAR RESEARCH

CERN-EP/2000-144
November 10, 2000

Measurements of the Cross Sections for Open Charm and Beauty Production in $\gamma\gamma$ Collisions at $\sqrt{s} = 189 - 202$ GeV

The L3 Collaboration

Abstract

The production of c and b quarks in $\gamma\gamma$ collisions is studied with the L3 detector at LEP with 410 pb^{-1} of data, collected at centre-of-mass energies from 189 GeV to 202 GeV. Hadronic final states containing c and b quarks are identified by detecting electrons or muons from their semileptonic decays. The cross sections $\sigma(e^+e^- \to e^+e^- c\bar{c}X)$ and $\sigma(e^+e^- \to e^+e^- b\bar{b}X)$ are measured and compared to next-to-leading order perturbative QCD calculations. The cross section of b production is measured in $\gamma\gamma$ collisions for the first time. It is in excess of the QCD prediction by a factor of three.

Submitted to *Phys. Lett. B*

1 Introduction

The measurement of heavy flavour production in two-photon collisions provides a reliable test of perturbative QCD because of the large physical scale set by the charm or beauty quark mass. Many experiments have studied charm production in $\gamma\gamma$ collisions [1, 2]. Beauty quark production in $\gamma\gamma$ collisions is expected to be suppressed by more than two orders of magnitude owing to its smaller electric charge and larger mass. At LEP energies, the direct and single resolved processes, shown in Figure 1, are predicted to give comparable contributions to the heavy flavour production cross section [3], whereas at low energies the direct process dominates. The main contribution to the resolved photon cross section is the photon-gluon fusion process $\gamma g \to c\bar{c}(b\bar{b})$. The production rate of c and b quarks in two-photon collisions therefore depends on their mass and the gluon density in the photon. Further contributions to charm production arise from the Vector Dominance Model (VDM) and from doubly resolved processes and are expected to be small.

This letter describes the measurements of the inclusive open charm and beauty production performed with the L3 detector [4] with 410 pb^{-1} of data, collected at centre-of-mass energies from 189 GeV to 202 GeV.

We identify b and c quarks by tagging electrons [1)] or muons from their semileptonic decays. Due to the higher mass of the b quarks, these leptons are characterized by a higher momentum and higher transverse momentum than those from c quarks. The $b\bar{b}$ production cross section is hence measured using the muon and electron transverse momentum spectra for both leptons having a momentum greater than 2 GeV. The charm cross section measurement is made by analysing the electron spectrum with momentum down to 0.6 GeV. Muons are always required to have a momentum greater than 2 GeV necessary to penetrate the calorimeters and reach the muon chambers.

2 Monte Carlo

The PYTHIA [5] Monte Carlo is used to model the two photon processes. The non-b events are generated with massless matrix elements [6] while for b events massive matrix elements are used. The resolved process uses the SaS1d photon structure function [7]. The two-photon luminosity function is implemented in the equivalent photon approximation (EPA) [8] with a cutoff $Q^2 < m_\rho^2$.

Background sources are $e^+e^- \to e^+e^-\tau^+\tau^-$, $e^+e^- \to Z/\gamma \to q\bar{q}$, $e^+e^- \to \tau^+\tau^-$ and $e^+e^- \to W^+W^-$. These processes are generated with JAMVG [9], PYTHIA, KORALZ [10] and KORALW [11] respectively. The detector simulation is performed using the GEANT [12] and GHEISHA [13] packages. The Monte Carlo events are reconstructed in the same way as the data. Time dependent detector inefficiencies, as monitored during the data taking period, are also simulated.

3 Event Selection Procedure

The event selection is performed in two steps. The first one selects hadronic final states produced in two-photon collisions, the second identifies a c or b quark by its semileptonic decay.

[1)] Electron stands for electron or positron throughout this paper.

3.1 Hadronic Two-Photon Events

Hadronic two-photon events are selected by requiring at least five tracks and a visible energy, $E_{\rm vis}$, below $\sqrt{s}/3$. The visible mass, $W_{\rm vis}$, of the event is calculated from the four-momentum vectors of the measured particles, tracks and calorimetric clusters including those from the small angle luminosity monitor. These particles are considered to be pions except for unmatched electromagnetic clusters considered as photons. $W_{\rm vis}$ has to be greater than 3 GeV. Figures 2a and 2b show the $E_{\rm vis}$ and $W_{\rm vis}$ distributions for the data compared with the Monte Carlo. The cut on $E_{\rm vis}$ separates the two-photon process from annihilation processes, characterized by high visible energy. The background from $\rm e^+e^- \to e^+e^-\tau^+\tau^-$ and $\rm e^+e^- \to \tau^+\tau^-$ events is suppressed by the requirement on the number of tracks.

The analysis is limited to untagged events with small photon virtuality. Events are excluded when the most energetic cluster in the small angle calorimeters has an energy greater than 0.2 $\sqrt{\rm s}$. Thus the interacting photons are quasi-real: $\langle \rm Q^2 \rangle \cong 0.015$ GeV^2, where $-\rm Q^2$ is the mass squared of the virtual photon.

3.2 Lepton Selection

Electrons from charm and beauty semileptonic decays are identified by requiring electromagnetic clusters in the polar angle range $|\cos\,\theta| < 0.725$ with momentum greater than 0.6 GeV. They should satisfy the following criteria:

- The candidate cluster is required to match to a track. The difference between the azimuthal angle between the shower barycentre and the track impact point at the calorimeter must be less than 20 mrad.
- The distribution of energies measured in the crystals of the calorimeter should be compatible with that of an electromagnetic cluster.
- The $\rm E_t/p_t$ ratio must be equal to one within 2σ, where $\rm E_t$ is the projection of the energy of the cluster on the plane transverse to the beam, $\rm p_t$ is the transverse momentum of the track and σ is the resolution on this ratio.
- Photon conversions are suppressed by requiring the distance of closest approach of the track to the mean $\rm e^+e^-$ collision point in the transverse plane to be less than 0.5 mm and the invariant mass of the electron candidate and of the closest track to be greater than 0.1 GeV.

After these cuts, 2434 events remain. The background from annihilation processes and two-photon production of tau pairs is estimated to be 0.75%.

Muon candidates are selected from tracks in the muon chambers in the angular range $|\cos\,\theta| < 0.8$. The momentum of the muons must be greater than 2.0 GeV. To suppress background from annihilation processes, the muon momentum must be less than 0.1 $\sqrt{\rm s}$. After all cuts are applied, 269 events remain. The estimated background from annihilation processes and two-photon production of tau pairs is 6.0%.

4 Total cross section $\boldsymbol{\sigma(\rm e^+e^- \to e^+e^-b\bar{b}X)}$

The b cross section is derived from a fit to the data distributions for events where the momentum of the muon or electron candidate is greater than 2.0 GeV, corresponding to 269 and 137 events

respectively. The b selection efficiency is 2.20% for muons and 1.25% for electrons. The transverse momentum of the lepton with respect to the nearest jet, P_t, is chosen as the fit variable since it has the highest sensitivity to the b fraction. The jets are reconstructed using the JADE algorithm [14] with $y_{cut} = 0.1$. The energy of the muon or electron is not included in the jet.

A χ^2 fit is performed to the data distributions using the sum of the Monte Carlo distributions of the non two-photon background N_{bkg}, light quark events N_{uds}, c quark events $N_{c\bar{c}}$ and b quark events $N_{b\bar{b}}$. A three parameter fit is applied in which the number of beauty, charm and light quarks are free parameters, whereas N_{bkg} is held fixed according to the Monte Carlo prediction. The results of the fit are given in Table 1 which shows also the charm cross section estimate from the fit of the muon and electron P_t spectra.

The fit for muons yields a b fraction of 51.6 ± 9.8 (stat) %. As for the electrons, the b fraction is 42.3 ± 11.4 (stat) %. The χ^2 per degree of freedom for the muon and electron fits are 6.2/6 and 10.1/6 respectively. If no b contribution is included in the fit, confidence levels of 2.2×10^{-5} and 1.2×10^{-3} are obtained for muon and electron respectively. The signal events are produced in two separate samples for direct and resolved processes assuming a 1:1 ratio [3]. The fitted distributions are shown in Figures 3 and 4.

The resulting cross sections for the luminosity averaged centre-of-mass energy $\langle\sqrt{s}\rangle = 194$ GeV are:

$$\sigma(e^+e^- \to e^+e^- b\bar{b}X)_{\text{muons}} = 14.9 \pm 2.8 \text{ (stat)} \ \pm 2.6 \text{ (syst) pb}$$
$$\sigma(e^+e^- \to e^+e^- b\bar{b}X)_{\text{electrons}} = 10.9 \pm 2.9 \text{ (stat)} \ \pm 2.0 \text{ (syst) pb.}$$

The systematic uncertainties arise from the event selection, jet reconstruction, massive or massless charm quarks in the event generation, b semileptonic branching ratio, trigger efficiency, Monte Carlo statistics and direct to resolved process ratio. Table 2 shows the values of systematic uncertainties due to these contributions. The dominant uncertainty comes from the event selection. It is estimated by variation of the cuts and includes detector resolution uncertainties and the agreement between data and Monte Carlo. The systematic uncertainty on jet reconstruction is assigned by variation of the y_{cut} parameter. The contribution due to the uncertainty on the ratio of the direct to the resolved processes is estimated by changing it from 1:1 to 1:2 or 2:1.

The combination of muon and electron results gives

$$\sigma(e^+e^- \to e^+e^- b\bar{b}X)_{\text{combined}} = 13.1 \pm 2.0 \text{ (stat)} \ \pm 2.4 \text{ (syst) pb.}$$

5 Total cross section $\sigma(e^+e^- \to e^+e^- c\bar{c}X)$

In order to increase the statistical accuracy for the charm cross section measurement, the electron momentum cut is relaxed from 2 GeV to 0.6 GeV. The cross section is calculated as for the data collected at centre-of mass energies from 91 GeV to 183 GeV [2]. In addition, the beauty contribution to the number of observed events is subtracted. The open charm cross section is then calculated from the number of events with leptons using the equation:

$$\sigma(e^+e^- \to e^+e^- c\bar{c}X) = \frac{(N^{\text{lept}}_{\text{obs}} - N^{\text{lept}}_{\text{bkg}} - N^{\text{lept}}_{\text{b}})\ \pi_c}{\mathcal{L}\ \epsilon_{\text{trig}}\ \epsilon'_c}, \tag{1}$$

where the variables are defined as follows:

- $N_{\rm obs}^{\rm lept}$ is the number of events in the data after the final electron selection (2434 events).
- $\epsilon_{\rm trig}$ is the trigger efficiency (94.4%) which is determined from the data using a set of independent triggers.
- $N_{\rm bkg}^{\rm lept}$ is the number of background events which do not originate from two-photon hadronic interactions estimated from Monte Carlo (18.3 ± 2.0 events).
- $N_{\rm b}^{\rm lept}$ is the number of beauty events (169.5) estimated from the cross section measured above.
- $\mathcal{L}$ is the total integrated luminosity (410 pb^{-1}).

The c selection efficiency, $\epsilon'_{\rm c}$, is the fraction of c events selected relative to those generated in the full phase space. In order to be independent of the Monte Carlo flavour composition, the charm purity is written as:

$$\pi_{\rm c} = (1 - \frac{\epsilon_{\rm uds}}{\epsilon_{\rm data}})/(1 - \frac{\epsilon_{\rm uds}}{\epsilon_{\rm c}}), \tag{2}$$

where $\epsilon_{\rm c}$ and $\epsilon_{\rm uds}$ are the fractions of charm events, $N_{\rm c}^{\rm lept}$, and light quark events, $N_{\rm uds}^{\rm lept}$, accepted by the final selection. Equation (2) follows from expressing the number of non-beauty hadronic events as:

$$\frac{N_{\rm c}^{\rm lept} + N_{\rm uds}^{\rm lept}}{\epsilon_{\rm data}} = \frac{N_{\rm c}^{\rm lept}}{\epsilon_{\rm c}} + \frac{N_{\rm uds}^{\rm lept}}{\epsilon_{\rm uds}}, \tag{3}$$

where the quantity $\epsilon_{\rm data}$ is defined by the following relation:

$$\epsilon_{\rm data} = \frac{N_{\rm c}^{\rm lept} + N_{\rm uds}^{\rm lept}}{N_{\rm c}^{\rm had} + N_{\rm uds}^{\rm had}} = \frac{N_{\rm obs}^{\rm lept} - N_{\rm bkg}^{\rm lept} - N_{\rm b}^{\rm lept}}{N_{\rm obs}^{\rm had} - N_{\rm bkg}^{\rm had} - N_{\rm b}^{\rm had}}. \tag{4}$$

$N_{\rm b}^{\rm had}$, $N_{\rm c}^{\rm had}$ and $N_{\rm uds}^{\rm had}$ are the number of hadronic events with b-quarks, c-quarks and light quarks respectively. $N_{\rm obs}^{\rm had}$ and $N_{\rm bkg}^{\rm had}$ are the observed number of hadronic events and the background expectations respectively. This method is insensitive to the absolute normalization of the c and uds background Monte Carlo samples, but still depends on the ratio of direct to resolved processes in the signal Monte Carlo.

For the electron sample, the charm purity is 75.0% and the charm selection efficiency is 0.41%. The charm production cross section in $\gamma\gamma$ collisions at $\langle\sqrt{s}\rangle = 194$ GeV is then:

$$\sigma(\mathrm{e^+e^-} \to \mathrm{e^+e^-c\bar{c}X})_{\rm electrons} = 1072 \pm 33 \text{ (stat) } \pm 126 \text{ (syst) pb.} \tag{5}$$

This charm cross section is compatible with the fit results reported in Table 1. The systematic uncertainties arise from the event selection, direct to resolved process ratio, c semileptonic branching ratio, massive or massless charm quarks in the event generation, experimental uncertainties on the beauty cross section, trigger efficiency, Monte Carlo statistics and uds background estimate. The average charm semileptonic branching ratio used in the simulation is 0.098 [15]. Table 3 shows the values of the systematic uncertainties due to different contributions. The dominant systematic uncertainty is from event selection and from the variation of the ratio of direct to resolved processes. They are estimated as in the beauty study.

The fit result for beauty production is checked by this counting method in the electron case, fixing the charm cross section to the value of equation (5). In addition to the momentum cut of 2 GeV, the transverse momentum $\mathrm{P_t}$ is required to be greater than 1.0 GeV. After all

cuts are applied 106 electron candidates remain. The beauty purity is 49.0%, and the selection efficiency is 1.2%. The cross section at $\langle\sqrt{s}\rangle = 194$ GeV is

$$\sigma(e^+e^- \to e^+e^- b\bar{b}X)_{\text{electrons}} = 11.3 \pm 2.3 \text{ (stat) pb},$$

in good agreement with the fit result.

Figure 5 shows the momentum distribution of the electron candidates. In this plot the charm and beauty cross sections predicted by the PYTHIA Monte Carlo are scaled to the measured values. The data and Monte Carlo shapes of the momentum distribution show a good agreement.

In the case of muons, where the 2 GeV cut can not be relaxed, the estimation of charm production is that derived by a simultaneous fit to the b and c fractions described in the previous section:

$$\sigma(e^+e^- \to e^+e^- c\bar{c}X)_{\text{muons}} = 814 \pm 164 \text{ (stat) } \pm 200 \text{ (syst) pb}$$

at $\langle\sqrt{s}\rangle = 194$ GeV. The efficiency is much lower for the muon sample, about 0.04%, due to the higher momentum cut. The dominant systematic uncertainties are the event selection and the direct to resolved process ratio.

The combined value for the open charm cross section at $\langle\sqrt{s}\rangle = 194$ GeV is:

$$\sigma(e^+e^- \to e^+e^- c\bar{c}X)_{\text{combined}} = 1016 \pm 30 \text{ (stat) } \pm 120 \text{ (syst) pb}.$$

6 Comparisons with QCD Predictions

The cross sections for open beauty and charm production are compared in Figure 6 to perturbative next-to-leading order QCD calculations [3]. The dashed line corresponds to the direct process, NLO QCD calculations, while the solid line shows the prediction for the sum of direct and resolved processes. The direct process depends upon the QCD coupling constant and the heavy-quark mass. The prediction for open charm is calculated using a charm mass of either 1.3 GeV or 1.7 GeV and the open charm threshold energy is set to 3.8 GeV. The theory prediction for the resolved process is calculated with the GRV parton density function [16]. The renormalization and factorization scales are chosen to be the heavy quark mass. The direct process $\gamma\gamma \to c\bar{c}$ is insufficient to describe the data, even if real and virtual gluon corrections are included. The data therefore require a significant gluon content in the photon.

The prediction for open beauty is calculated for a b quark mass of 4.5 GeV or 5.0 GeV and the open beauty threshold energy is set to 10.6 GeV. For $\langle\sqrt{s}\rangle = 194$ GeV and a b quark mass of 4.5 GeV, this cross section is 4.4 pb. The $b\bar{b}$ cross section is measured in $\gamma\gamma$ collisions for the first time and is a factor of 3 and about 4 statistical uncertainty standard deviations higher than expected.

Acknowledgements

We wish to express our gratitude to the CERN accelerator divisions for the excellent performance of the LEP machine. We also acknowledge and appreciate the effort of the engineers, technicians and support staff who have participated in the construction and maintenance of this experiment.

References

[1] JADE Collab., W. Bartel *et al.,* Phys. Lett. **B 184** (1987) 288,
TPC/Two-Gamma Collab., M. Alston-Garnjost *et al.,* Phys. Lett. **B 252** (1990) 499.
TASSO Collab., W. Braunschweig *et al.,* Z. Phys. **C 47** (1990) 499.
TOPAZ Collab., R. Enomoto *et al.,* Phys. Lett. **B 328** (1994) 535; Phys. Rev. **D 50** (1994) 1879; Phys. Lett. **B 341** (1994) 99; Phys. Lett. **B 341** (1994) 238.
VENUS Collab., S. Uehara *et al.,* Z. Phys. **C 63** (1994) 213.
AMY Collab., T. Aso *et al.,* Phys. Lett. **B 363** (1995) 249; Phys. Lett. **B 381** (1996) 372.
ALEPH Collab., D. Buskulic *et al.,* Phys. Lett. **B 355** (1995) 595.

[2] L3 Collab., M. Acciarri *et al.*, Phys. Lett. **B 453** (1999) 83;
A. Stone, *Measurement of inclusive charm production in two-photon collisions at LEP*, thesis submitted to Louisiana State University (1999).

[3] M. Drees *et al.*, Phys. Lett. **B 306** (1993) 371.

[4] L3 Collab., B. Adeva *et al.*, Nucl. Inst. Meth. **A 289** (1990) 35;
M. Acciarri *et al.*, Nucl. Inst. Meth. **A 351** (1994) 300;
M. Chemarin *et al.*, Nucl. Inst. Meth. **A 349** (1994) 345;
I.C. Brock *et al.*, Nucl. Inst. Meth. **A 381** (1996) 236;
A. Adam *et al.*, Nucl. Inst. Meth. **A 383** (1996) 342.

[5] PYTHIA version 5.722 is used.
T. Sjöstrand, Preprint CERN-TH/7112/93 (1993), revised August 1995; Comp. Phys. Comm. **82** (1994) 74.

[6] M. Cacciari *et al.,* Nucl. Phys. **B 466** (1996) 173.

[7] G.A. Schuler and T. Sjöstrand, Z. Phys. **C 68** (1995) 607; Phys. Lett. **B 376** (1996) 193.

[8] V.M. Budnev *et al.,* Phys. Rep. **15** (1975) 181.

[9] J.A.M. Vermaseren, Nucl. Phys. **B 229** (1983) 347.

[10] KORALZ version 4.02 is used.
S. Jadach, B.F.L. Ward and Z. Wąs, Comp. Phys. Comm. **79** (1994) 503.

[11] KORALW version 1.33 is used.
S. Jadach *et al.,* Comp. Phys. Comm. **94** (1996) 216;
S. Jadach *et al.,* Phys. Lett. **B 372** (1996) 289.

[12] GEANT version 3.15 is used.
R. Brun *et al.*, Preprint CERN DD/EE/84-1 (1984), revised 1987.

[13] H. Fesefeldt, RWTH Aachen Report PITHA 85/2 (1985).

[14] JADE Collab., W. Bartel *et al.,* Z. Phys. **C 33** (1986) 23;
JADE Collab., S. Bethke *et al.,* Phys. Lett. **B 213** (1988) 235.

[15] ALEPH, DELPHI, L3 and OPAL Collab., Nucl. Inst. Meth. **A 378** (1996) 101.

[16] M. Glück, E. Reya and A. Vogt, Phys. Rev. **D 46** (1992) 1973.

Author List

The L3 Collaboration:

M.Acciarri,[26] P.Achard,[19] O.Adriani,[16] M.Aguilar-Benitez,[25] J.Alcaraz,[25] G.Alemanni,[22] J.Allaby,[17] A.Aloisio,[28] M.G.Alviggi,[28] G.Ambrosi,[19] H.Anderhub,[49] V.P.Andreev,[6,36] T.Angelescu,[12] F.Anselmo,[9] A.Arefiev,[27] T.Azemoon,[3] T.Aziz,[10] P.Bagnaia,[35] A.Bajo,[25] L.Baksay,[44] A.Balandras,[4] S.V.Baldew,[2] S.Banerjee,[10] Sw.Banerjee,[10] A.Barczyk,[49,47] R.Barillère,[17] P.Bartalini,[22] M.Basile,[9] N.Batalova,[46] R.Battiston,[32] A.Bay,[22] F.Becattini,[16] U.Becker,[14] F.Behner,[49] L.Bellucci,[16] R.Berbeco,[3] J.Berdugo,[25] P.Berges,[14] B.Bertucci,[32] B.L.Betev,[49] S.Bhattacharya,[10] M.Biasini,[32] A.Biland,[49] J.J.Blaising,[4] S.C.Blyth,[33] G.J.Bobbink,[2] A.Böhm,[1] L.Boldizsar,[13] B.Borgia,[35] D.Bourilkov,[49] M.Bourquin,[19] S.Braccini,[19] J.G.Branson,[40] F.Brochu,[4] A.Buffini,[16] A.Buijs,[45] J.D.Burger,[14] W.J.Burger,[32] X.D.Cai,[14] M.Capell,[14] G.Cara Romeo,[9] G.Carlino,[28] A.M.Cartacci,[16] J.Casaus,[25] G.Castellini,[16] F.Cavallari,[35] N.Cavallo,[37] C.Cecchi,[32] M.Cerrada,[25] F.Cesaroni,[23] M.Chamizo,[19] Y.H.Chang,[51] U.K.Chaturvedi,[18] M.Chemarin,[24] A.Chen,[51] G.Chen,[7] G.M.Chen,[7] H.F.Chen,[20] H.S.Chen,[7] G.Chiefari,[28] L.Cifarelli,[39] F.Cindolo,[9] C.Civinini,[16] I.Clare,[14] R.Clare,[38] G.Coignet,[4] N.Colino,[25] S.Costantini,[5] F.Cotorobai,[12] B.de la Cruz,[25] A.Csilling,[13] S.Cucciarelli,[32] T.S.Dai,[14] J.A.van Dalen,[30] R.D'Alessandro,[16] R.de Asmundis,[28] P.Déglon,[19] A.Degré,[4] K.Deiters,[47] D.della Volpe,[28] E.Delmeire,[19] P.Denes,[34] F.DeNotaristefani,[35] A.De Salvo,[49] M.Diemoz,[35] M.Dierckxsens,[2] D.van Dierendonck,[2] C.Dionisi,[35] M.Dittmar,[49] A.Dominguez,[40] A.Doria,[28] M.T.Dova,[18,♯] D.Duchesneau,[4] D.Dufournaud,[4] P.Duinker,[2] I.Duran,[41] H.El Mamouni,[24] A.Engler,[33] F.J.Eppling,[14] F.C.Erné,[2] A.Ewers,[1] P.Extermann,[19] M.Fabre,[47] M.A.Falagan,[25] S.Falciano,[35,17] A.Favara,[17] J.Fay,[24] O.Fedin,[36] M.Felcini,[49] T.Ferguson,[33] H.Fesefeldt,[1] E.Fiandrini,[32] J.H.Field,[19] F.Filthaut,[17] P.H.Fisher,[14] I.Fisk,[40] G.Forconi,[14] K.Freudenreich,[49] C.Furetta,[26] Yu.Galaktionov,[27,14] S.N.Ganguli,[10] P.Garcia-Abia,[5] M.Gataullin,[31] S.S.Gau,[11] S.Gentile,[35,17] N.Gheordanescu,[12] S.Giagu,[35] Z.F.Gong,[20] G.Grenier,[24] O.Grimm,[49] M.W.Gruenewald,[8] M.Guida,[39] R.van Gulik,[2] V.K.Gupta,[34] A.Gurtu,[10] L.J.Gutay,[46] D.Haas,[5] A.Hasan,[29] D.Hatzifotiadou,[9] T.Hebbeker,[8] A.Hervé,[17] P.Hidas,[13] J.Hirschfelder,[33] H.Hofer,[49] G. Holzner,[49] H.Hoorani,[33] S.R.Hou,[51] Y.Hu,[30] I.Iashvili,[48] B.N.Jin,[7] L.W.Jones,[3] P.de Jong,[2] I.Josa-Mutuberría,[25] R.A.Khan,[18] D.Käfer,[1] M.Kaur,[18,◇] M.N.Kienzle-Focacci,[19] D.Kim,[35] J.K.Kim,[43] J.Kirkby,[17] D.Kiss,[13] W.Kittel,[30] A.Klimentov,[14,27] A.C.König,[30] M.Kopal,[46] A.Kopp,[48] V.Koutsenko,[14,27] M.Kräber,[49] R.W.Kraemer,[33] W.Krenz,[1] A.Krüger,[48] A.Kunin,[14,27] P.Ladron de Guevara,[25] I.Laktineh,[24] G.Landi,[16] M.Lebeau,[17] A.Lebedev,[14] P.Lebrun,[24] P.Lecomte,[49] P.Lecoq,[17] P.Le Coultre,[49] H.J.Lee,[8] J.M.Le Goff,[17] R.Leiste,[48] P.Levtchenko,[36] C.Li,[20] S.Likhoded,[48] C.H.Lin,[51] W.T.Lin,[51] F.L.Linde,[2] L.Lista,[28] Z.A.Liu,[7] W.Lohmann,[48] E.Longo,[35] Y.S.Lu,[7] K.Lübelsmeyer,[1] C.Luci,[17,35] D.Luckey,[14] L.Lugnier,[24] L.Luminari,[35] W.Lustermann,[49] W.G.Ma,[20] M.Maity,[10] L.Malgeri,[17] A.Malinin,[17] C.Maña,[25] D.Mangeol,[30] J.Mans,[34] G.Marian,[15] J.P.Martin,[24] F.Marzano,[35] K.Mazumdar,[10] R.R.McNeil,[6] S.Mele,[17] L.Merola,[28] M.Meschini,[16] W.J.Metzger,[30] M.von der Mey,[1] A.Mihul,[12] H.Milcent,[17] G.Mirabelli,[35] J.Mnich,[1] G.B.Mohanty,[10] T.Moulik,[10] G.S.Muanza,[24] A.J.M.Muijs,[2] B.Musicar,[40] M.Musy,[35] M.Napolitano,[28] F.Nessi-Tedaldi,[49] H.Newman,[31] T.Niessen,[1] A.Nisati,[35] H.Nowak,[48] R.Ofierzynski,[49] G.Organtini,[35] A.Oulianov,[27] C.Palomares,[25] D.Pandoulas,[1] S.Paoletti,[35,17] P.Paolucci,[28] R.Paramatti,[35] H.K.Park,[33] I.H.Park,[43] G.Passaleva,[17] S.Patricelli,[28] T.Paul,[11] M.Pauluzzi,[32] C.Paus,[17] F.Pauss,[49] M.Pedace,[35] S.Pensotti,[26] D.Perret-Gallix,[4] B.Petersen,[30] D.Piccolo,[28] F.Pierella,[9] M.Pieri,[16] P.A.Piroué,[34] E.Pistolesi,[26] V.Plyaskin,[27] M.Pohl,[19] V.Pojidaev,[27,16] H.Postema,[14] J.Pothier,[17] D.O.Prokofiev,[46] D.Prokofiev,[36] J.Quartieri,[39] G.Rahal-Callot,[49,17] M.A.Rahaman,[10] P.Raics,[15] N.Raja,[10] R.Ramelli,[49] P.G.Rancoita,[26] R.Ranieri,[16] A.Raspereza,[48] G.Raven,[40] P.Razis,[29] D.Ren,[49] M.Rescigno,[35] S.Reucroft,[11] S.Riemann,[48] K.Riles,[3] J.Rodin,[44] B.P.Roe,[3] L.Romero,[25] A.Rosca,[8] S.Rosier-Lees,[4] S.Roth,[1] C.Rosenbleck,[1] J.A.Rubio,[17] G.Ruggiero,[16] H.Rykaczewski,[49] S.Saremi,[6] S.Sarkar,[35] J.Salicio,[17] E.Sanchez,[17] M.P.Sanders,[30] C.Schäfer,[17] V.Schegelsky,[36] S.Schmidt-Kaerst,[1] D.Schmitz,[1] H.Schopper,[50] D.J.Schotanus,[30] G.Schwering,[1] C.Sciacca,[28] A.Seganti,[9] L.Servoli,[32] S.Shevchenko,[31] N.Shivarov,[42] V.Shoutko,[27] E.Shumilov,[27] A.Shvorob,[31] T.Siedenburg,[1] D.Son,[43] B.Smith,[33] P.Spillantini,[16] M.Steuer,[14] D.P.Stickland,[34] A.Stone,[6] B.Stoyanov,[42] A.Straessner,[1] K.Sudhakar,[10] G.Sultanov,[18] L.Z.Sun,[20] S.Sushkov,[8] H.Suter,[49] J.D.Swain,[18] Z.Szillasi,[44,¶] T.Sztaricskai,[44,¶] X.W.Tang,[7] L.Tauscher,[5] L.Taylor,[11] B.Tellili,[24] C.Timmermans,[30] Samuel C.C.Ting,[14] S.M.Ting,[14] S.C.Tonwar,[10] J.Tóth,[13] C.Tully,[17] K.L.Tung,[7] Y.Uchida,[14] J.Ulbricht,[49] E.Valente,[35] G.Vesztergombi,[13] I.Vetlitsky,[27] D.Vicinanza,[39] G.Viertel,[49] S.Villa,[11] M.Vivargent,[4] S.Vlachos,[5] I.Vodopianov,[36] H.Vogel,[33] H.Vogt,[48] I.Vorobiev,[33] A.A.Vorobyov,[36] A.Vorvolakos,[29] M.Wadhwa,[5] W.Wallraff,[1] M.Wang,[14] X.L.Wang,[20] Z.M.Wang,[20] A.Weber,[1] M.Weber,[1] P.Wienemann,[1] H.Wilkens,[30] S.X.Wu,[14] S.Wynhoff,[17] L.Xia,[31] Z.Z.Xu,[20] J.Yamamoto,[3] B.Z.Yang,[20] C.G.Yang,[7] H.J.Yang,[7] M.Yang,[7] J.B.Ye,[20] S.C.Yeh,[52] An.Zalite,[36] Yu.Zalite,[36] Z.P.Zhang,[20] G.Y.Zhu,[7] R.Y.Zhu,[31] A.Zichichi,[9,17,18] G.Zilizi,[44,¶] B.Zimmermann,[49] M.Zöller.[1]

1 I. Physikalisches Institut, RWTH, D-52056 Aachen, FRG[§]
III. Physikalisches Institut, RWTH, D-52056 Aachen, FRG[§]
2 National Institute for High Energy Physics, NIKHEF, and University of Amsterdam, NL-1009 DB Amsterdam, The Netherlands
3 University of Michigan, Ann Arbor, MI 48109, USA
4 Laboratoire d'Annecy-le-Vieux de Physique des Particules, LAPP,IN2P3-CNRS, BP 110, F-74941 Annecy-le-Vieux CEDEX, France
5 Institute of Physics, University of Basel, CH-4056 Basel, Switzerland
6 Louisiana State University, Baton Rouge, LA 70803, USA
7 Institute of High Energy Physics, IHEP, 100039 Beijing, China[△]
8 Humboldt University, D-10099 Berlin, FRG[§]
9 University of Bologna and INFN-Sezione di Bologna, I-40126 Bologna, Italy
10 Tata Institute of Fundamental Research, Bombay 400 005, India
11 Northeastern University, Boston, MA 02115, USA
12 Institute of Atomic Physics and University of Bucharest, R-76900 Bucharest, Romania
13 Central Research Institute for Physics of the Hungarian Academy of Sciences, H-1525 Budapest 114, Hungary[‡]
14 Massachusetts Institute of Technology, Cambridge, MA 02139, USA
15 KLTE-ATOMKI, H-4010 Debrecen, Hungary[¶]
16 INFN Sezione di Firenze and University of Florence, I-50125 Florence, Italy
17 European Laboratory for Particle Physics, CERN, CH-1211 Geneva 23, Switzerland
18 World Laboratory, FBLJA Project, CH-1211 Geneva 23, Switzerland
19 University of Geneva, CH-1211 Geneva 4, Switzerland
20 Chinese University of Science and Technology, USTC, Hefei, Anhui 230 029, China[△]
22 University of Lausanne, CH-1015 Lausanne, Switzerland
23 INFN-Sezione di Lecce and Università Degli Studi di Lecce, I-73100 Lecce, Italy
24 Institut de Physique Nucléaire de Lyon, IN2P3-CNRS,Université Claude Bernard, F-69622 Villeurbanne, France
25 Centro de Investigaciones Energéticas, Medioambientales y Tecnologícas, CIEMAT, E-28040 Madrid, Spain[♭]
26 INFN-Sezione di Milano, I-20133 Milan, Italy
27 Institute of Theoretical and Experimental Physics, ITEP, Moscow, Russia
28 INFN-Sezione di Napoli and University of Naples, I-80125 Naples, Italy
29 Department of Natural Sciences, University of Cyprus, Nicosia, Cyprus
30 University of Nijmegen and NIKHEF, NL-6525 ED Nijmegen, The Netherlands
31 California Institute of Technology, Pasadena, CA 91125, USA
32 INFN-Sezione di Perugia and Università Degli Studi di Perugia, I-06100 Perugia, Italy
33 Carnegie Mellon University, Pittsburgh, PA 15213, USA
34 Princeton University, Princeton, NJ 08544, USA
35 INFN-Sezione di Roma and University of Rome, "La Sapienza", I-00185 Rome, Italy
36 Nuclear Physics Institute, St. Petersburg, Russia
37 INFN-Sezione di Napoli and University of Potenza, I-85100 Potenza, Italy
38 University of Californa, Riverside, CA 92521, USA
39 University and INFN, Salerno, I-84100 Salerno, Italy
40 University of California, San Diego, CA 92093, USA
41 Dept. de Fisica de Particulas Elementales, Univ. de Santiago, E-15706 Santiago de Compostela, Spain
42 Bulgarian Academy of Sciences, Central Lab. of Mechatronics and Instrumentation, BU-1113 Sofia, Bulgaria
43 Laboratory of High Energy Physics, Kyungpook National University, 702-701 Taegu, Republic of Korea
44 University of Alabama, Tuscaloosa, AL 35486, USA
45 Utrecht University and NIKHEF, NL-3584 CB Utrecht, The Netherlands
46 Purdue University, West Lafayette, IN 47907, USA
47 Paul Scherrer Institut, PSI, CH-5232 Villigen, Switzerland
48 DESY, D-15738 Zeuthen, FRG
49 Eidgenössische Technische Hochschule, ETH Zürich, CH-8093 Zürich, Switzerland
50 University of Hamburg, D-22761 Hamburg, FRG
51 National Central University, Chung-Li, Taiwan, China
52 Department of Physics, National Tsing Hua University, Taiwan, China
§ Supported by the German Bundesministerium für Bildung, Wissenschaft, Forschung und Technologie
‡ Supported by the Hungarian OTKA fund under contract numbers T019181, F023259 and T024011.
¶ Also supported by the Hungarian OTKA fund under contract numbers T22238 and T026178.
♭ Supported also by the Comisión Interministerial de Ciencia y Tecnología.
♯ Also supported by CONICET and Universidad Nacional de La Plata, CC 67, 1900 La Plata, Argentina.
♢ Also supported by Panjab University, Chandigarh-160014, India.
△ Supported by the National Natural Science Foundation of China.

Fit results	Muon Tag	Electron Tag
N_{bkg}	16.2 (fixed)	2.9 (fixed)
$N_{b\bar{b}}$	126.7 ± 24.1	52.5 ± 14.1
$N_{c\bar{c}}$	119.0 ± 24.0	71.5 ± 14.8
N_{uds}	$0.0^{+33.0}_{-\ 0.0}$	$0.0^{+7.4}_{-0.0}$
χ^2 / d.o.f.	6.2 / 6	10.1 / 6
$\sigma(e^+e^- \to e^+e^-b\bar{b}X)$, (pb)	14.9 ± 2.8	10.9 ± 2.9
$\sigma(e^+e^- \to e^+e^-c\bar{c}X)$, (pb)	814 ± 164	1092 ± 226

Table 1: Fit to the distribution of the transverse momentum of the lepton with respect to the nearest jet. The fit parameters are constrained to be positive. The correlation between $N_{b\bar{b}}$ and $N_{c\bar{c}}$ is 75%.

Source of uncertainty	Muon Tag	Electron Tag
	$\Delta\sigma(e^+e^- \to e^+e^-b\bar{b}X)$, %	$\Delta\sigma(e^+e^- \to e^+e^-b\bar{b}X)$, %
Event selection	14.6	15.8
Jet reconstruction	8.2	8.2
Massive/massless charm	3.0	3.0
$B(b \to e, \mu)$	2.0	2.0
Trigger efficiency	2.0	2.0
Monte Carlo statistics	1.4	1.8
Direct / resolved ratio	1.0	0.9
Total	17.3	18.4

Table 2: Systematic uncertainties on $\sigma(e^+e^- \to e^+e^-b\bar{b}X)$.

Source of uncertainty	Electron Tag	Muon Tag
	$\Delta\sigma(e^+e^- \to e^+e^-c\bar{c}X)$, %	$\Delta\sigma(e^+e^- \to e^+e^-c\bar{c}X)$, %
Event selection	8.5	18.6
Direct / resolved ratio	5.7	10.9
B($c \to e, \mu$)	3.0	5.0
Massive/massless charm	3.0	3.0
b background	2.4	—
Trigger efficiency	2.0	2.0
Monte Carlo statistics	1.9	6.0
uds background	1.1	—
Jet reconstruction	—	8.2
Total	11.7	24.6

Table 3: Systematic uncertainties on $\sigma(e^+e^- \to e^+e^-c\bar{c}X)$.

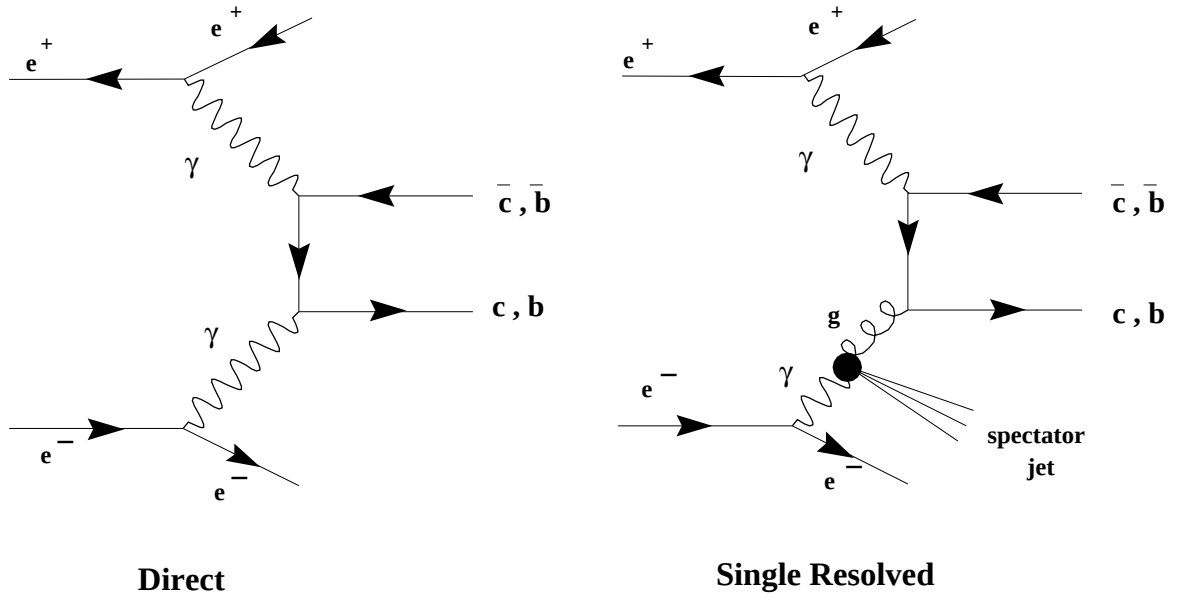

Figure 1: Diagrams contributing to charm and beauty production in $\gamma\gamma$ collisions at LEP.

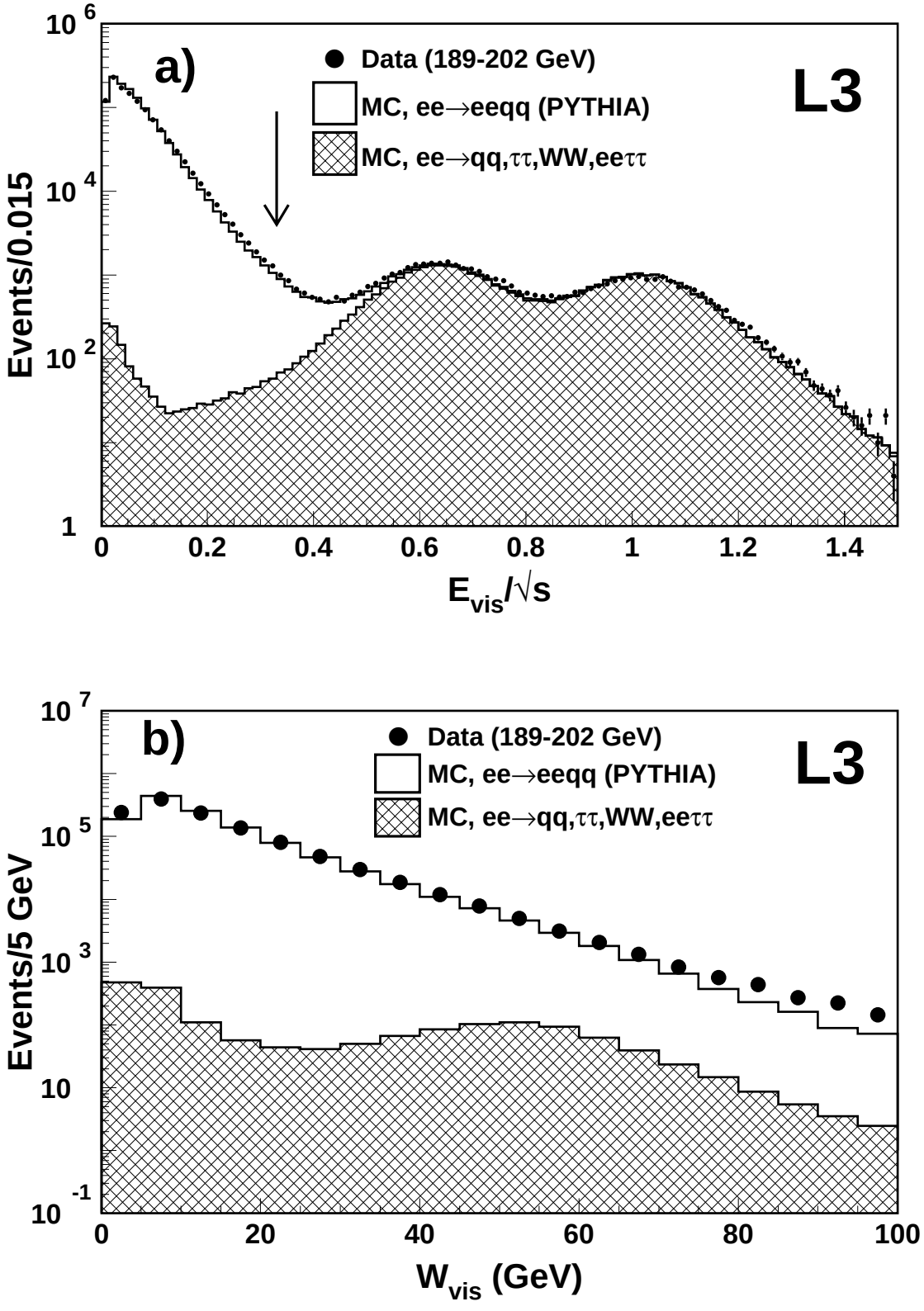

Figure 2: a) Total visible energy after applying hadronic selection cuts. A cut of $E_{\rm vis} < 0.33\sqrt{s}$ indicated by the arrow removes most of the backgrounds. b) The visible mass after applying hadronic selection cuts.

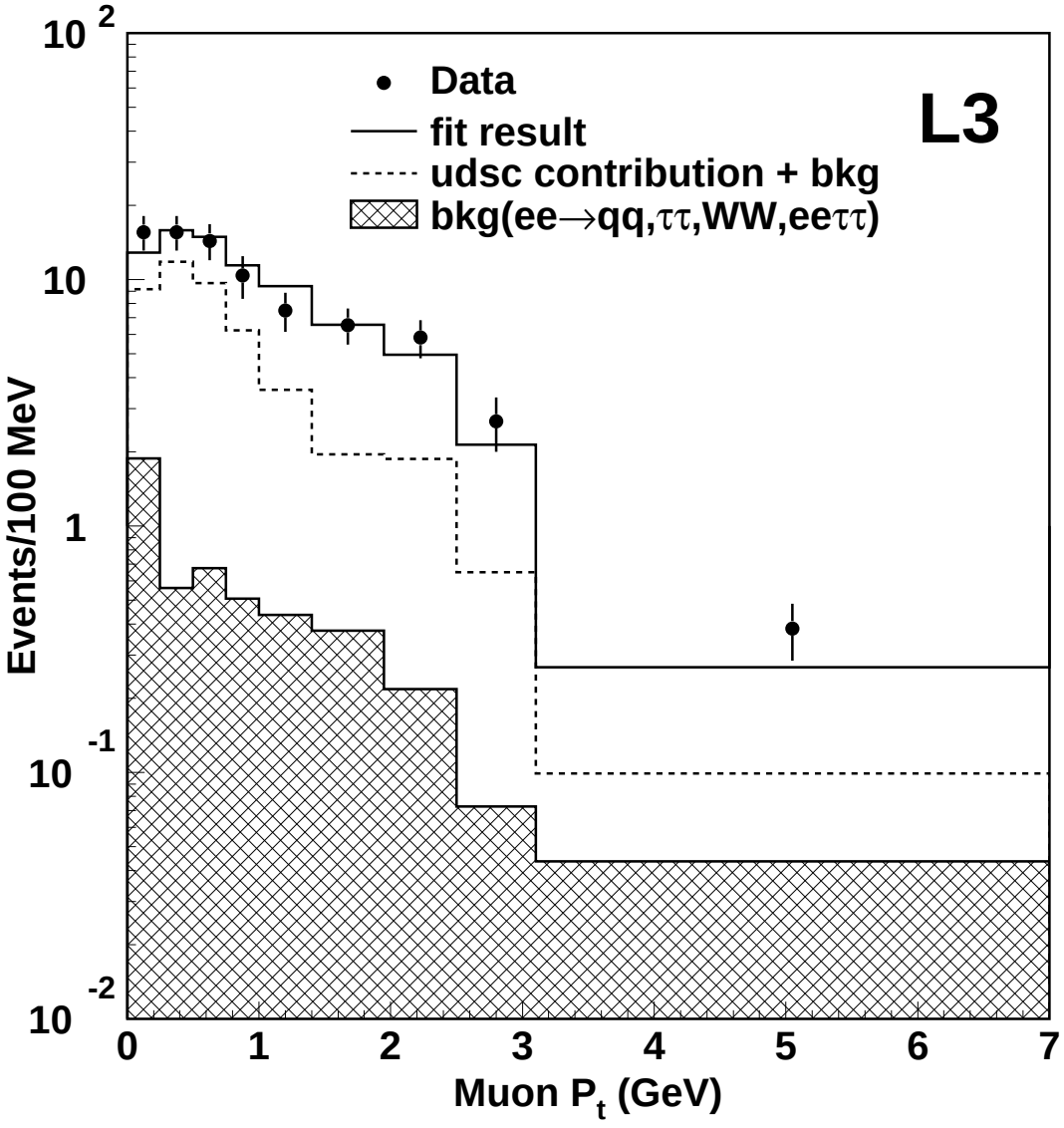

Figure 3: The distribution of the transverse momentum, P_t, of the muon candidate with respect to the closest jet.

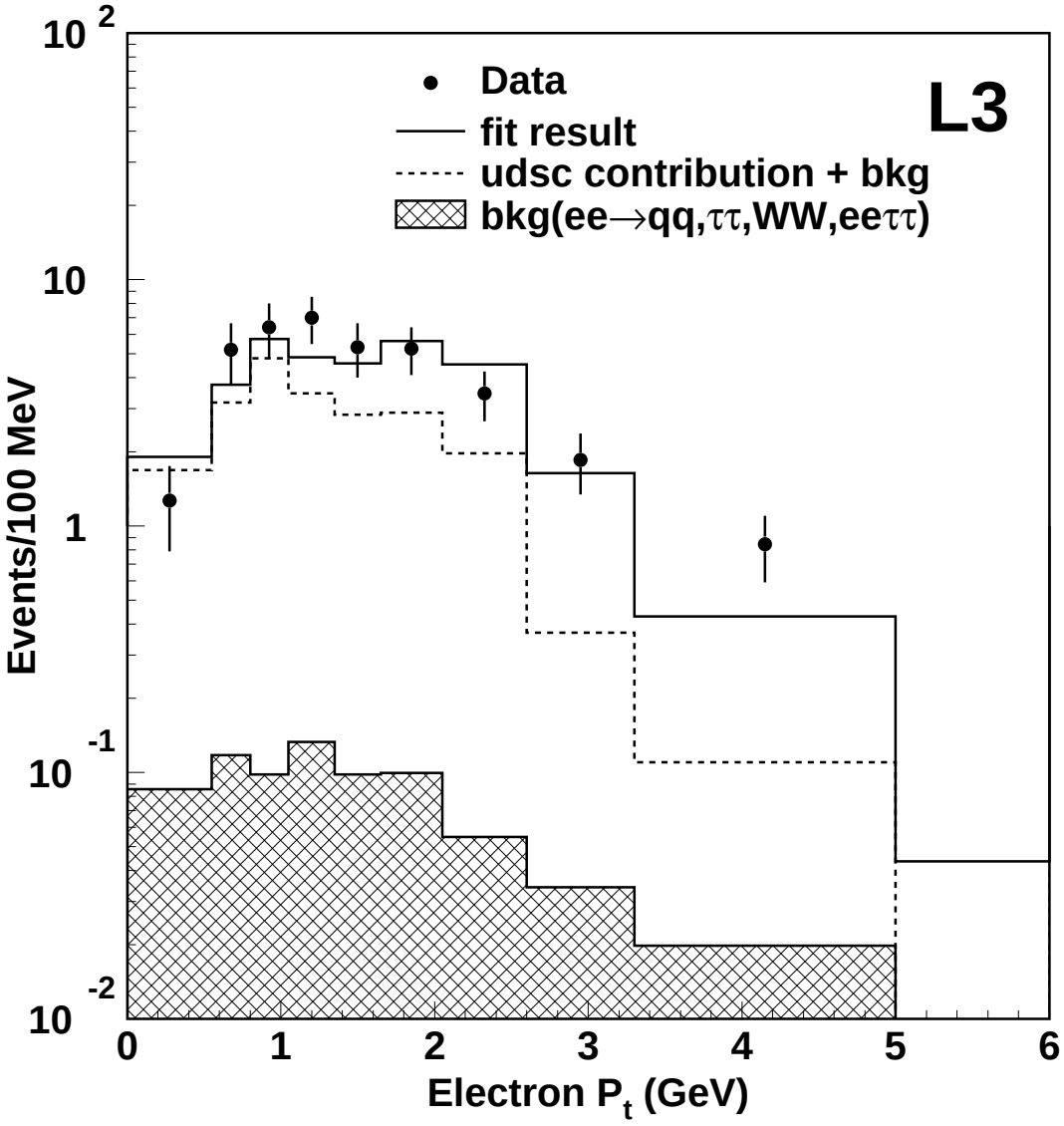

Figure 4: The distribution of the transverse momentum, P_t, of the electron candidate with respect to the closest jet.

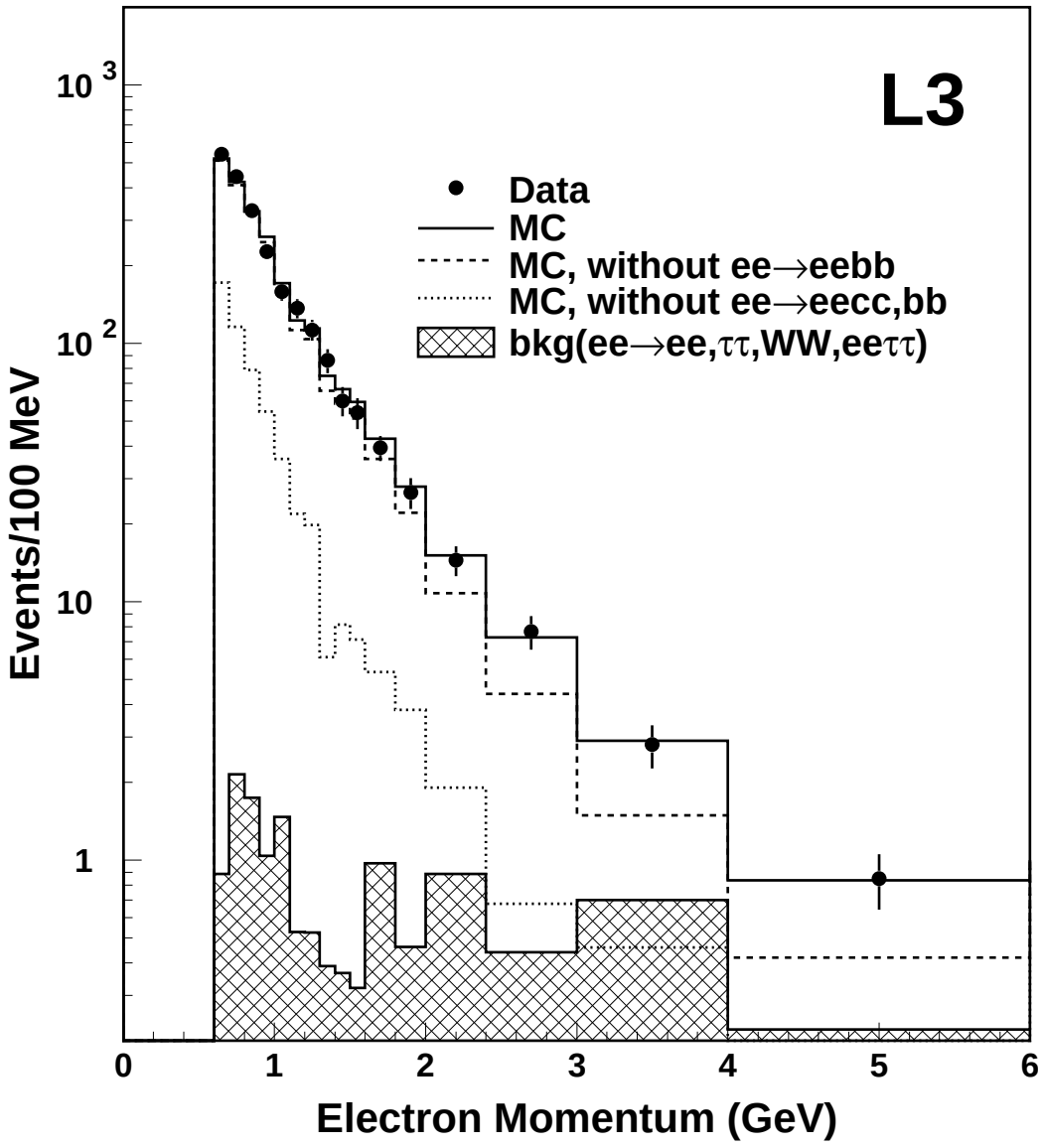

Figure 5: The momentum of the electron candidates. The dotted, dashed and solid histograms are the contributions of uds, udsc and udscb quarks from the PYTHIA Monte Carlo. The c and b fraction of PYTHIA are scaled to the measured cross sections.

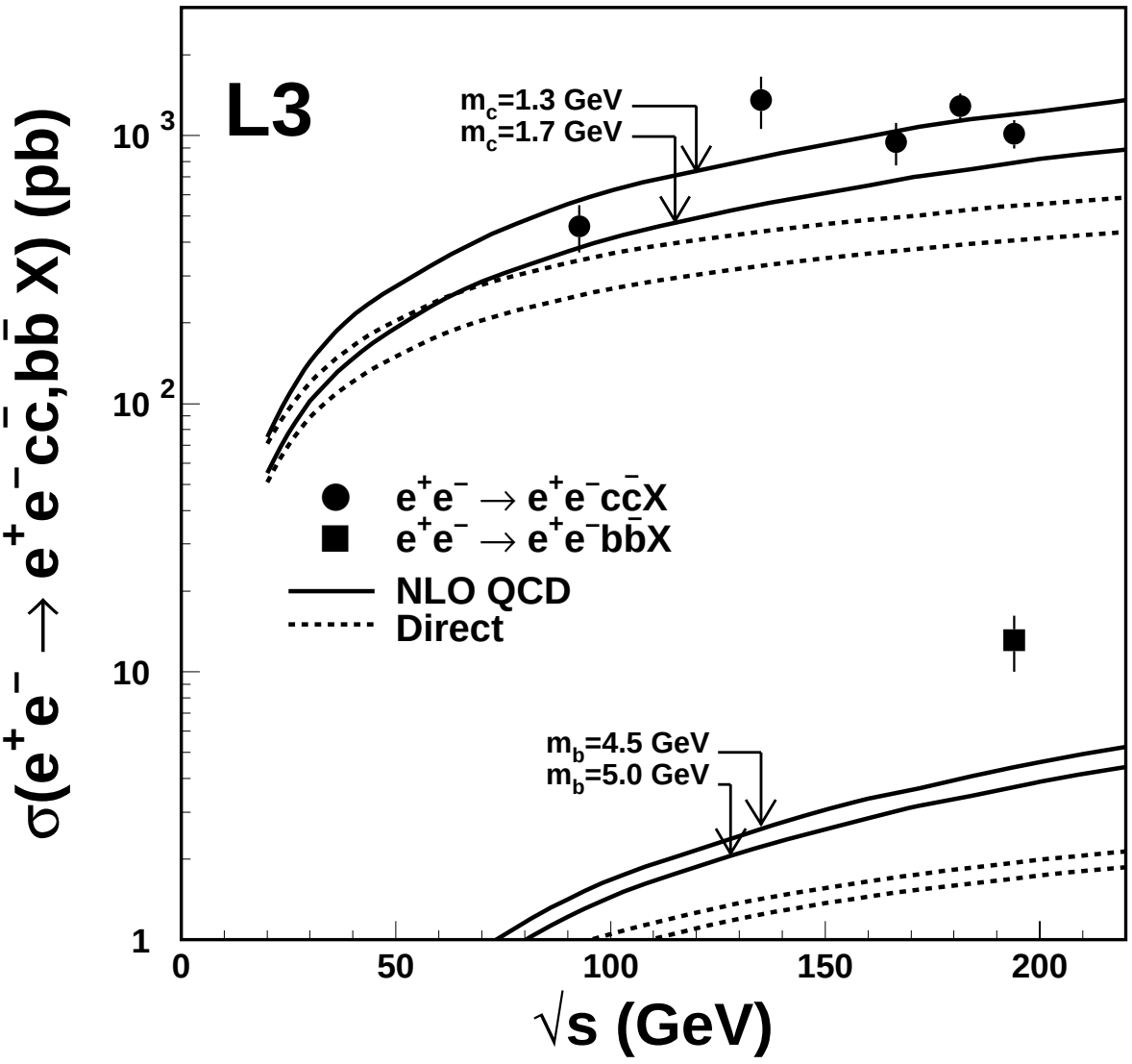

Figure 6: The open charm and beauty production cross section in two-photon collisions. The L3 data from both electron and muon events are combined. The statistical and systematic uncertainties are added in quadrature. The dashed line corresponds to the direct process contribution and the solid line represents the NLO QCD prediction for the sum of the direct and resolved processes.